Review

Progress in the Separation and Purification of Carbon Hydrocarbon Compounds Using MOFs and Molecular Sieves

Yousheng Zhou [1], Peicheng Li [1], Yifan Wang [1], Qiyue Zhao [1] and Hui Sun [1,2,3,*]

1   School of Chemical Engineering, East China University of Science and Technology, Shanghai 200237, China; y30220197@mail.ecust.edu.cn (Y.Z.); y30220236@mail.ecust.edu.cn (P.L.); y30220056@mail.ecust.edu.cn (Y.W.); y20220012@mail.ecust.edu.cn (Q.Z.)
2   International Joint Research Center of Green Energy Chemical Engineering, East China University of Science and Technology, Shanghai 200237, China
3   Ministry Key Laboratory of Oil and Gas Fine Chemicals, School of Chemical Engineering and Technology, Xinjiang University, Urumqi 830046, China
*   Correspondence: sunhui@ecust.edu.cn; Tel.: +86-21-64252916

Abstract: Carbon hydrocarbon compounds, especially low-carbon hydrocarbons (C_1–C_3), are vital raw materials in the petrochemical industry, but their efficient separation has great challenges due to their similar molecular structures and properties. In contrast to traditional low-temperature distillation and absorption separation technologies, selective adsorption employing porous materials as adsorbent has the advantages of low energy consumption, high efficiency, and high selectivity, indicating broad application possibilities in the field of low-carbon hydrocarbon separation. In this paper, the recent progress in the separation and purification of hydrocarbon mixtures by means of the two kinds of porous materials (metal–organic frameworks and molecular sieves) that have been widely used in recent years is reviewed, including purification of methane and separation of ethylene/ethane, propylene/propane, and some high-carbon hydrocarbon isomers. The structure–activity relationships between their chemical composition, structural characteristics, and separation performance are discussed to understand the separation mechanism. In conclusion, the issues encountered in the application of metal–organic frameworks and molecular sieves in the separation of low-carbon hydrocarbons are discussed in light of the current context of "carbon neutrality".

Keywords: adsorption separation; low-carbon hydrocarbons; metal–organic framework; molecular sieve; pore structure

1. Introduction

Natural gas, oilfield associated gas, coalbed methane, biogas, and other low-carbon hydrocarbon mixtures (C_1–C_3) are high-quality energy and chemical raw materials [1,2]. Natural gas, particularly methane (CH_4), plays an essential role in reducing energy consumption and preventing environmental deterioration and is predicted to become the primary source of global energy by 2030 [3,4]. Ethylene (C_2H_4) and propylene (C_3H_6) are in high demand as the primary raw materials for synthetic polymers such as polyethylene, polyvinyl chloride, and polypropylene. In 2021, the global production capacity of ethylene and propylene exceeded 214 million tons and 120 million tons, respectively [5,6]. However, due to the presence of impurities (CO_2, various trace gases, etc.), the optimum purity (>99.5%) cannot be attained in the manufacturing and transportation of low-carbon hydrocarbons, which limits the economic benefits and corrodes pipes, thus producing environmental contamination [7,8]. Therefore, to improve long-term growth and application, it is crucial to develop effective and affordable low-carbon hydrocarbon separation and purification technology.

Table 1 shows that the physicochemical properties of low-carbon hydrocarbon molecules are remarkably similar, making separation challenging. In industry, high

purity goods are frequently obtained at the expense of high equipment expenditures and energy usage (about 15% of world energy demand) [9,10]. Cryogenic distillation, a common separation procedure, primarily utilizes the difference in the boiling points of molecules to separate the target products. However, this approach relies on a large number of trays and on high reflux; this has the disadvantages of being expensive and consuming a lot of energy [11]. Furthermore, solvent absorption is a typical approach that relies on the solubility of gas in the absorbent for separation. However, the addition of various solvents complicates the separation process by triggering solvent regeneration and solvent loss issues [12].

Table 1. Physical properties of $C_1 \sim C_3$ light hydrocarbons [9,13].

Adsorbate	Boiling Point (K)	Dynamic Diameter (Å)	Dipole Moment ($\times 10^{18}$/ ESU cm)	Polarizability ($\times 10^{-25}$/cm^3)
CH_4	111.6	3.8	0	25.9
CO_2	194.6	3.3	0	2.76
N_2	77.15	3.6	0	1.53
C_2H_6	184.6	4.4	0	44.3
C_2H_4	169.4	4.2	0	42.5
C_3H_8	231.0	4.3–5.1	0.084	62.9
C_3H_6	225.5	4.7	0.366	62.9

In comparison to the energy-driven distillation process, adsorption separation technology consumes less than one third of the energy and is simple to operate. Meanwhile, material selectivity guidance-based structural control can achieve extraordinarily high separation precision [9,14,15]. Metal–organic frameworks (MOFs) and molecular sieves are the most extensively utilized adsorption and separation materials in the field of carbon hydrocarbon separation. The diversity of their topologies and the designability of their pore structures have aroused the scientific community's interest. MOFs are porous organic–inorganic hybrid materials with large specific surface area, multi-metal sites, customizable structure, and numerous modification methods. They could be used to precisely identify tiny differences in structural properties, such as the polarity and unsaturation of low-carbon hydrocarbon molecules, which is now a widespread issue [16]. Because of their sturdy construction, simple preparation process, and low cost, molecular sieves are widely utilized in the petrochemical industry and they also exhibit outstanding performance in the separation of low-carbon hydrocarbons [17]. They each have their own set of advantages and disadvantages. MOFs, a novel multidisciplinary porous material, are projected to boost the separation selectivity and adsorption capacity of low-carbon hydrocarbons to new heights, with enormous promise and broad possibilities. However, the cost of MOFs is prohibitively high, and more research into practical applications is required. In comparison to MOFs, molecular sieves are more stable structurally and have lower costs for raw ingredients, making them more suitable for industrial development. However, the molecular sieve's pore size distribution, specific surface area, and surface functionalization are constrained by its design.

This article reviews the latest progress of metal–organic frameworks and molecular sieves as selective adsorbents in the separation of carbon hydrocarbon compounds, especially low-carbon hydrocarbons, with the aim of providing guidance for the development of more stable, efficient, and low-cost adsorption materials in the future. It primarily consists of methane purification (methane and nitrogen and methane and carbon dioxide), ethylene and ethane separation, and propylene and propane separation. Adsorption and separation mechanisms are explored, as well as the structure–activity relationship between pore structure, chemical properties, separation selectivity, and adsorption capacity (Figure 1). In order to upgrade the adsorption separation system, the use of high-carbon hydrocarbon isomer separation, which differs from low-carbon hydrocarbon separation, is briefly introduced. Finally, the challenges and future development of these two adsorbents

in the field of separation and purification of carbon hydrocarbon compounds are explored in the context of carbon neutrality.
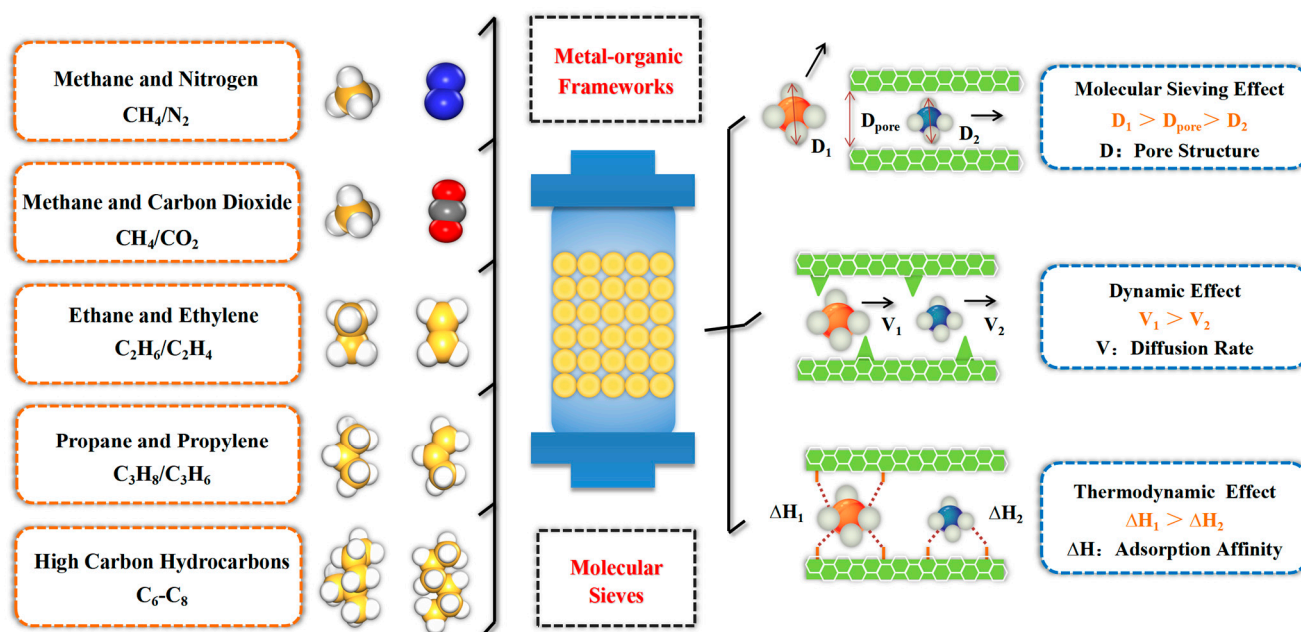
Figure 1. Research abstract of adsorption separation materials in the field of low-carbon hydrocarbon purification and separation.

2. Separation Mechanism of Low-Carbon Hydrocarbons

The internal diffusion of gas in adsorbent particles is the important stage in determining whether it can be adsorbed in the separation and purification of low-carbon hydrocarbons [18]. At the same time, the structural properties of low-carbon hydrocarbons differ in terms of molecular polarity, molecule size, and degree of matching with adsorbents. To summarize, the separation mechanism of low-carbon hydrocarbons can be divided into three types [11,19,20]: (i) molecular sieve effect, which is primarily determined by molecular size and the shape, size, and pore structure of the adsorbent matching degree, as well as the mismatch of molecules for exclusion; (ii) kinetic effect, which influences separation performance based on the varied diffusion speeds of distinct gas molecules in the adsorbent; and (iii) thermodynamic equilibrium effect, particular interaction between distinct gas molecules and adsorbents, better separation selectivity can be attained by this specific recognition process.

The metal–organic framework can be built and regulated using the aforesaid separation mechanism [21,22]: (i) controlling the pore volume, pore diameter, and other pore features in the action site space; (ii) introducing a metal component, creating a strong action site in the pore, and improving the interaction between the gas molecule and the adsorbent; and (iii) adding polar components to the adsorbent's surface. Organic/inorganic ligands can be used to functionalize metal–organic frameworks and introduce polar groups onto the pore surface.

The effect of molecular gates can be used on a wide range of molecular sieves, including carbon and zeolite molecular sieves, and the pore size can be precisely adjusted using acid, alkali, light, heat treatment, ion exchange, or loading to become close to the target molecular size for separation. Furthermore, metal ions can be used to modify or functionalize molecular sieves, giving them the features and functionality of recognizing certain molecules [23–26].

3. Purification of Methane

Methane is abundantly dispersed in nature, and it is frequently employed as a fuel (such as coal gas, natural gas, and so on) in civil industry. Because of its low C/H ratio, methane can lower CO_2 concentration after combustion, making it a promising clean energy source [27]. However, due to its complicated sources, it contains impurities including N_2, CO_2, trace gases, and other contaminants. These impurities not only lower the calorific value of methane, but also produce pipeline pollution during transportation, which has a major impact on the environment. As a result, efficient methane gas separation can improve the economic and social benefits of practical significance.
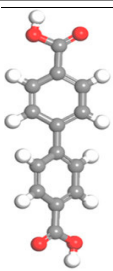
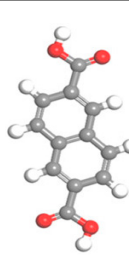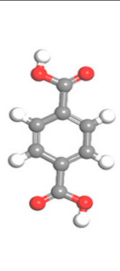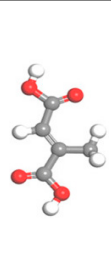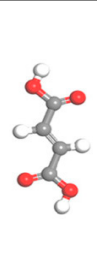### 3.1. Adsorption Separation of Methane and Nitrogen

One of the major sources of methane production is coalbed methane, a type of unconventional natural gas that is stored in coal seams and is mostly made up of CH_4, N_2, and CO_2 [28]. The methane content in the coal seam can be greatly reduced by the injection of massive volumes of air (70% nitrogen) during underground mining, making it unsuitable for use as a fuel and chemical [29]. Every year, between 20 and 29 billion cubic meters of coalbed methane is emitted into the atmosphere, resulting in significant energy waste [30]. Methane/nitrogen separation and purification can help to alleviate energy shortages to some extent.
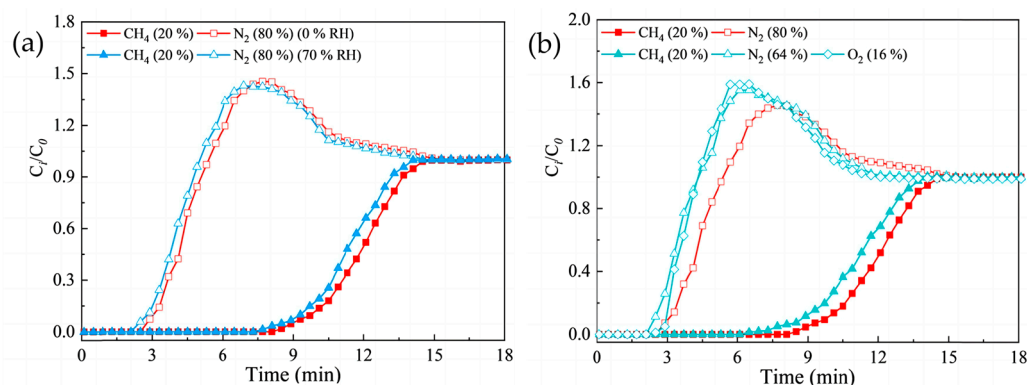
3.1.1. Metal–Organic Frameworks for Methane/Nitrogen Separation

It is challenging to distinguish between CH_4 (3.8 Å) and N_2 (3.6 Å) because of their similar molecular sizes. However, compared to N_2, the adsorption binding point distance between CH_4 and MOFs is shorter and the adsorption affinity is larger. In this scenario, controlling the pore size of MOFs is a good method of separation. To produce high CH_4/N_2 separation selectivity and high CH_4 uptake, researchers frequently altered the pore size and pore surface chemical property by adjusting the ligand size, length, and polarity [31]. Chang et al. [32] synthesized a series of meshed aluminum-based MOFs with varying ligand sizes and polarity. As shown in Table 2, although Al-FUM-Me was weaker in terms of ligand polarity than Al-FUM, the existence of tiny pore size allowed it to demonstrate rational adsorption selectivity that was higher than that of many zeolite and carbon adsorption materials (8.6). The data also suggested that channel size was critical for CH_4 separation, and that CH_4 uptake was connected to a synergistic effect of pore size and ligand polarity, not just one of them. Furthermore, breakthrough studies (Figure 2a,b) revealed that the adsorbent exhibited good regeneration and structural stability while entirely separating CH_4 and N_2, serving as a model for the development of future MOFs adsorbents. Wang et al. [33] created four nickel-based diamond ligand networks from pyridine carboxylic acid bifunctional ligands of varying lengths and functional groups. The CH_4/N_2 selectivity (15.8) and CH_4 uptake (40.8 cm^3/g) of Ni(ina)$_2$ were significantly better than those reported in the literature, which provided a new standard for the adsorption and separation of MOFs. Although the pore size of the material was similar to that of Al-FUM-Me, there were four possible CH_4 binding sites in the pore and several interactions (C-H$\cdots\pi$) with the pyridine ring adjacent, which had stronger adsorption affinity for CH_4 molecule. The comparison also demonstrated how MOFs could effectively increase the separation performance by combining the molecular sieve effect with the thermodynamic equilibrium effect. Additionally, altering or tweaking the MOFs' ligands could improve the materials' stability while also improving their adsorption capacity. Li et al. [34] used 1,4-NDC (1,4-naphthalene dicarboxylic acid) and ADC (9,10-anthracene dicarboxylic acid) to replace BDC ligand on DMOF, and introduced non-polar aromatic ring to shield Zn-O bond so as to change the moisture resistance of DMOF, so that it could maintain stability in humid environment, and also provided new ideas for designing efficient and stable adsorption materials in the future.

Table 2. Polarity and pore size of aluminum-based MOFs materials [32].

| Name	Al-BPDC	Al-NDC	Al-BDC	Al-FUM-Me	Al-FUM
Ligand Structure					
Ligand Polarity (kcal/mol)	10.683	10.729	11.467	12.585	14.291
Aperture (Å)	11.5	9.2	8.2	5.0	6.3
CH_4 Uptake (cm^3/g)	5.9	10.86	15.98	27.19	20.44
CH_4/N_2 Selectivity	2.2	3.1	3.4	8.6	5.1

Figure 2. Breakthrough experimental results of Al-FUM-Me under real environmental conditions. (**a**) CH_4/N_2 (20/80) mixture with a humidity of 70% RH and (**b**) CH_4/N_2/O_2 (20/64/16) mixture under ambient conditions. Republished from ref. [32], copyright (2022), with permission from ACS.

3.1.2. Molecular Sieves for Methane/Nitrogen Separation

ETS-4 molecular sieve and CHA zeolite are two extensively used commercial adsorbents in the separation and purification of methane, and their tunable eight-membered ring structure and matching pore size indicate good potential in CH_4 and N_2 separation [35]. However, their small pore size limits their adsorption capacity and selectivity to some extent, making separation performance difficult to demonstrate [36]. Yang et al. [37] created a "doughnut-shaped" meso-micro layered K-Chabazite (CHA-type molecular sieve) nanocrystal based on this. The CH_4 uptake through the newly designed pore and diffusion channel was as high as 40.12 cm^3/g, indicating good industrial potential. In contrast to conventional CH_4/N_2 separation adsorbents, our group developed a series of Sr-ETS-4 samples employing N_2 as a potent adsorbent through heat treatment and ion exchange [38]. The findings of molecular modeling and adsorption isotherms (Figure 3a–c) demonstrated that the thermal stability, nitrogen adsorption rate, and adsorption capacity of Sr-ETS-4 all increase as the degree of Sr ion exchange rises. This adsorbent was more suited to treating natural gas that contains more CH_4 than N_2, which helped to increase economic benefits and offers fresh approaches to the separation and purification of methane. Carbon molecular sieve (CMS) is also a useful fundamental substance for separating CH_4 and N_2, due to its acid, alkali, and heat resistance. The modification strategy based on thermodynamic equilibrium effect can considerably improve the adsorption and separation performance of carbon molecular sieve [39]. Yang et al. [40] found that the CH_4 uptake of

poly ethylene imine (PEI) modified coal-based carbon molecular sieve (CMS-P-N) prepared in nitrogen could reach 6.76 mmol/g. Zhang et al. [41] used chemical vapor deposition with benzene as the deposition agent to create a carbon molecular sieve (CMS) from cobalt and nickel impregnated carbonaceous material precursors, and its CH_4/N_2 kinetic selectivity could reach 35.26. Although the effect of the aforementioned modification method was remarkable, as adsorption time increases, some micropores may be covered and blocked by deposited coke, resulting in poor adsorption performance, which was also an urgent problem to be solved in the future modification of carbon molecular sieves.
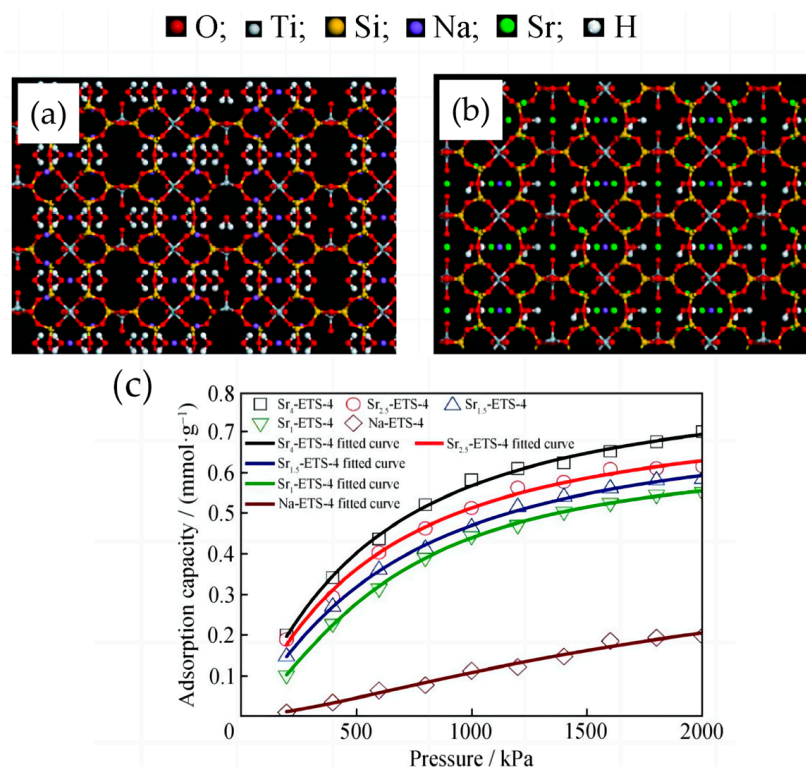
Figure 3. Structural models of ETS-4 and simulated adsorption isotherms of nitrogen on Na-ETS-4 and Sr-ETS-4. (**a**) Na-ETS-4, (**b**) Sr-ETS-4, and (**c**) simulated adsorption isotherms of nitrogen on Na-ETS-4 and Sr-ETS-4 [38].
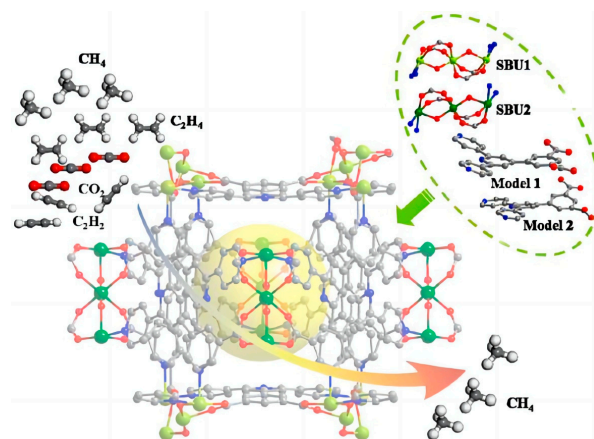
3.2. Adsorption Separation of Methane and Carbon Dioxide

Biogas and landfill gas are composed of 35–70% CH_4 and 15–40% CO_2 [42]. Decarbonization is required to achieve high purity CH_4 (>97%). However, the decarbonization cost must account for 20–30% of the entire cost, which is incompatible with large-scale production and contradicts the promoted "double-carbon" strategy, which is not conducive to industry and energy structure adjustment. Exploring an efficient and cost-effective way to decarbonization is thus an urgent problem that must be addressed [43].

3.2.1. Metal–Organic Frameworks for Methane/Carbon Dioxide Separation

Designing a porous material with a diameter between CO_2 and CH_4 is one of the most successful ways to separate them since there is a subtle variation in their molecular dynamics diameters (CO_2: 3.3 Å to CH_4: 3.8 Å). Additionally, CO_2 has a greater contact with the surface of MOFs due to its increased quadrupole moment [44,45]. Under these conditions, it is possible to successfully encourage the separation of CO_2 and CH_4 by improving the contact between the guest molecule and its host spine [46]. These techniques, including adding high-density metal open sites (OMSs), doping polar groups, and altering the acidity and polarity of porous environments to promote host–guest interaction have shown positive results based on the aforementioned molecular sieve effect and thermo-

dynamic equilibrium [47]. Chen et al. [48] altered Ni-MOF-74 by adding -CH_3, -NH_2, -F, and -O-Li groups. DFT and GGA simulations demonstrated that the addition of the-O-Li group in LI-O-Ni-MOF-74 modified the electrostatic potential gradient distribution surrounding the material, which impacted the interaction between the material and CO_2 with a high quadrupole moment. Furthermore, the microstructure study revealed that the specific surface area and pore volume of Li-O-Ni-MOF-74 were 162.03% and 86.42% greater, respectively, than those of Ni-MOF-74, demonstrating that Li-O-Ni-MOF-74 had a higher adsorption capability. Zhang et al. [49] created a nano cage-based Fe-MOF with open metal sites (OMSs) and ideal pore space, with a distance of 3.8 Å between the outer cage and the open window hole in the inner cage. Each cage was also linked to six adjacent cages along the a-axis direction (as shown in Figure 4), and its pore screening effect had unique recognizability for small molecule gases, resulting in good methane and carbon dioxide separation performance, with CO_2/CH_4 selectivity reaching 16.7. Zheng et al. [50] investigated the high porosity and excellent water stability of MOFs while developing the subject–object interaction, and a water-stable acyl amide functionalized MOF (HNUST-8) with these three features was created. The breakthrough experimental results showed that CH_4 was detected in approximately 8 min and CO_2 in about 22 min, demonstrating the practicability of CO_2/CH_4 adsorption and separation while maintaining MOF stability.

Figure 4. Schematic diagram of nanocage-based Fe–MOF structure. Republished from ref. [49], copyright (2020), with permission from ACS.

3.2.2. Molecular Sieves for Methane/Carbon Dioxide Separation

In the separation of methane and carbon dioxide, zeolite molecular sieves and carbon molecular sieves are widely used as adsorbents. While zeolite molecular sieves, such as 13X and zeolite 5A, demonstrate superior separation performance under low pressure conditions (below 0.2 MPa), carbon molecular sieves offer the advantage of lower regeneration energy consumption. Conversely, under high pressure conditions (above 0.2 MPa), carbon molecular sieves exhibit better enhancement of methane purity, making them more favorable for the separation of these two gases [51,52]. A key strategy for CH_4 and CO_2 separation using carbon molecular sieves is the regulation of pore structure [53]. Liang et al. [54] utilized coconut shell carbonization material as a raw material and prepared carbon molecular sieves through a steam activation process. The study revealed that under the most suitable conditions, the CO_2/CH_4 equilibrium adsorption separation coefficient could reach 10.27. However, as the activation reaction was intensified, the microporous walls were further burned, resulting in the formation of macropores and a decrease in CH_4 adsorption. This phenomenon further emphasizes the significance of pore structure in the separation performance of carbon molecular sieves. Kaya et al. [55] produced carbon molecular sieves from defatted waste coffee grounds using $ZnCl_2$ and benzene, resulting in a pore size distribution of approximately 0.343 nm. Orlando et al. [56] utilized polyurethane (PU) as a carbon source to produce activated carbon for the preparation of carbon molecular

sieves, with pore sizes smaller than 0.37 nm, matching the separation of size for CO_2 and CH_4. These methods of preparing carbon molecular sieves through the recycling and utilization of waste materials not only provide innovative approaches for methane decarbonization but also hold significant implications for mitigating global carbon emissions. However, further research is required to investigate the stability of adsorbent materials and their practical applications before they can be considered suitable for large-scale industrial separation operations.

4. Adsorption Separation of Olefins and Alkanes

Olefins play a vital role as bulk raw materials in the production of various high-value-added chemicals, including polyethylene, polyvinyl chloride, and polypropylene. The global market value of ethylene and propylene is projected to reach USD 47.58 billion by 2023, with a continuous increase in demand [57]. However, the industrial production process of ethylene and propylene inevitably introduces impurities such as ethane and propane [58]. The separation of olefins and paraffins, characterized by their remarkably similar molecular structures and sizes, is widely recognized as one of the seven separations that have the potential to revolutionize the world. It is worth noting that the industrial separation of ethylene and ethane alone accounts for 0.3% of the world's energy consumption [59]. Therefore, the development of suitable and efficient adsorbent separation materials holds immense strategic value and significance in driving energy-saving initiatives and achieving carbon peak and carbon neutrality [60].

4.1. Adsorption Separation of Ethylene and Ethane

Ethylene, frequently referred to as the industry's "lifeblood" is essential to the petrochemical industry. In 2021, the rise of the new energy industry has further stimulated the ethylene demand market [61]. The two main industrial processes for producing ethylene at the moment are catalytic cracking of light hydrocarbons and steam cracking of naphtha [59]. However, these procedures are not entirely effective and frequently lead to the appearance of ethane impurities, which affect the processing of future polymer products and jeopardize the purity of ethylene. As a result, it is thought necessary to purify and separate ethylene and ethane.

4.1.1. Metal–Organic Frameworks for Ethylene/Ethane Separation

The efficacy of metal–organic frameworks and molecular sieves in separating ethylene and ethane from other adsorption materials is excellent, as demonstrated in Table 3. Metal–organic frameworks, backed by their high surface area and pore volume, ordered crystal structure, and tunable pore environment, demonstrate significant potential for gas storage and separation, particularly with the combination of high adsorption capacity and separation selectivity. The existence of a π-π double bond in ethylene, which ethane lacks, allows it to create strong connections with open metal cation sites despite their structural similarity. Unsaturated coordinating metals are frequently added to MOF materials to improve the separation selectivity of C_2H_4/C_2H_6 [62–64]. AgM-DS, a more stable Ag(I) π-complex adsorbent, was created by Yin et al. [65] by mixing $AgNO_3$ with the traditional metal–organic framework (MOF) MIL-101 via a dual-solvent method (as shown in Figure 5). Because MIL-101 has a smaller pore volume than the $AgNO_3$ solution produced by this method, capillary forces may induce it to bind to the hydrophilic nanocavities of MOFs, so limiting the metal sites. This leads to a C_2H_4 uptake that can reach 75.5 cm^3/g. The pore structure of MOFs can be altered in order to improve the separation efficiency of C_2H_4/C_2H_6.

Table 3. Summary of some adsorption separation materials in C_2H_4 and C_2H_6 separation at 100 kPa.

| Adsorbents		T (K)	C_2H_4 Uptake (mmol/g)	C_2H_6 Uptake (mmol/g)	Selectivity		Qst (C_2H_4/C_2H_6, kJ mol^{-1})	Ref.
					C_2H_4/C_2H_6	C_2H_6/C_2H_4		
MOFs	UTSA-280	298	2.5	0.098	>10,000	-	34.1/-	[47]
	Fe-MOF-74	318	6.24	5.19	13.6	-	45/25	[47]
	ZIF-7	298	1.90	2.00	-	2.5	-/27	[47]
	MUF-15	298	4.15	4.69	-	1.96	-/29.2	[47]
	Co-gallate	298	3.37	0.31	52	-	44/-	[66]
	JNU-2	298	3.62	4.11	-	1.6	-/30	[67]
Zeolites	DDR	303	0.94	0.97	-	1.49	-/25	[62]
	Silicalite-1	305	1.84	2.00	-	2.90	-/28.9	[62]
	Ag-Ca-4A	298	3.7	-	17,568	-	-	[68]
	ITQ-55	303	1.30 [a]	0.80 [b]	6.36	-	-	[69]
COFs	COF-102	298	1.73	1.90		1.48	-/28.9	[62]
	COF-320	298	1.79	2.35	-	1.52	-/28.0	[62]
	CTF-DCTC-400	298	1.68	1.82	-	1.04	-/22.7	[62]
Carbon-Based Adsorbents	MC-S-Ag-3	298	3.4	2.6	2.4	-	-	[17]
	C-PDA-3	298	5.1	6.6	1.83	-	22/22	[17]
	CuCl(8.0)/AC	303	2.6	0.7	69.4	-	-	[17]
	MGA-750–3	298	5.68	7.02	-	2.00	28.4/-	[62]
	FAU-ZTC	303	3.86	4.71	-	1.48	25.0/-	[62]

a. Pressure at 45 kPa; b. Pressure at 60 kPa.
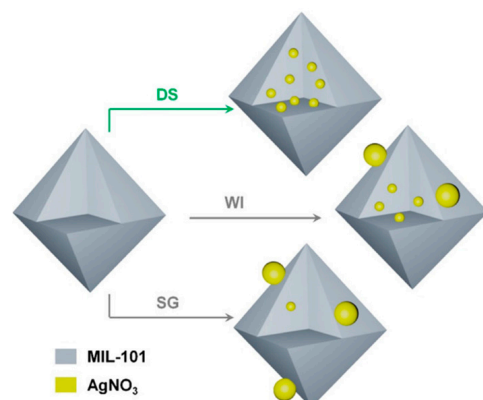
Figure 5. Decoration of AgNO$_3$ on MIL-101 using three methods: DS (upper route), wet-impregnation (middle route), and solid-phase grinding (lower route). Republished from ref. [65], copyright (2020), with permission from ACS.

Bao et al. [66] produced a number of mixed metal–organic framework materials based on terephthalate esters, which deviates from the conventional research link between kinetic diameter and pore structure. The 3D-linked zigzag channels in M-terephthalate esters (M = Ni, Mg, and Co) have pore diameters that are appropriate for separating ethylene from ethane based on molecular cross-sectional size rather than kinetic diameter. IAST selectivity for C_2H_4/C_2H_6 can be up to 52. Additionally, the majority of adsorbents preferentially absorb ethylene, but the co-adsorption phenomena make the desorption process energy intensive. Hence, the creation of porous materials that emphasize the separation of ethane and demonstrate superior performance has significant potential and has emerged as a recent focal point in research. Zeng et al. [67] took into consideration the impact of humidity on the adsorbent and devised JNU-2, which showcased great separation performance even in humid environments while prioritizing C_2H_6 adsorption. Di et al. [70] fabricated a one-dimensional hexagonal nonpolar pore surface MOF material, FJI-H11-Me (des), comprised aromatic rings and alkyl groups (as depicted in Figure 6d). Breakthrough experimental results (Figure 6a–c) reveal that FJI-H11Me (des) sustains excellent separation performance under varying gas flow rates, temperatures, and relative

humidity conditions. It can produce 99.95% pure polymer-grade C_2H_4 in a single step, opening up new perspectives and separation methods for ethylene and ethane in the future.
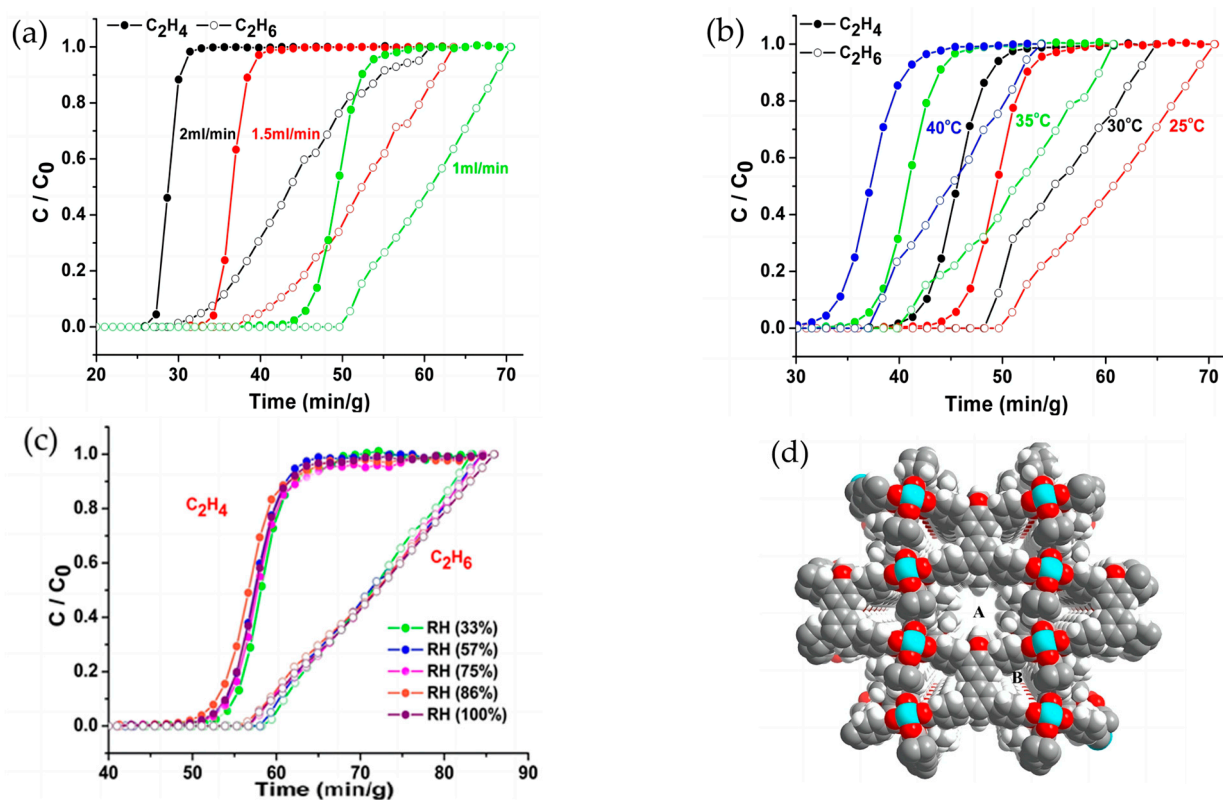

Figure 6. Experimental column breakthrough curves for a C_2H_6/C_2H_4 (*v/v*, 1/99) mixture in an absorber bed packed with FJI-H11-Me(des): (**a**) an experiment with FJI-H11-Me(des) under different gas flow rates, (**b**) the experiment of FJI-H11-Me(des) under different temperatures with gas flow rate of the 1 mL/min, (**c**) The experiment of FJI-H11-Me(des) under different relative humidity with gas flow rate of the 1 mL/min, and (**d**) FJI-H11-Me(des) one-dimensional hexagonal non-polar pore structure diagram. Republish from ref. [70], copyright (2022), with permission from Wiley.

4.1.2. Molecular Sieves for Ethylene/Ethane Separation

In the separation of ethylene and ethane, zeolites primarily utilize thermodynamic equilibrium separation mechanisms (π-complexation) and zeolite sieving mechanisms (pore structure regulation) [26]. Among them, LTA-type and FAU-type zeolites have shown high separation performance [71,72]. In recent years, researchers have often employed ion exchange methods to modify the structural properties of zeolites for further improvement of olefin/paraffin separation. Ilonavan et al. [73] conducted ethylene adsorption tests using single-metal-modified zeolites (K-A, Na-A, and Ca-A) with different ion radii, demonstrating the influence of pore size on adsorption performance. Liu et al. [68] prepared Ag-Ca-4A samples by adjusting 4A zeolite with bimetallic ions. This sample combines thermodynamic equilibrium and zeolite mechanisms, exhibiting precise size matching and specific recognition sites, with a high C_2H_4 uptake of 3.7 mmol/g.

Our group used tandem fixed beds to link two ion-exchanged LTA zeolites for the separation of C_3H_6 and C_2H_4 from a four-component gas mixture ($C_2H_4/C_2H_6/C_3H_6/C_3H_8$) (as shown in Figure 7a). This connection method first sets up two adsorbers (filled with Ni-5A and Ag-Cd-4A, respectively) in series, and introduces a mixture of ethylene, propylene, and alkane to adsorb propylene and ethylene; Afterwards, these two adsorbers were set in parallel and desorption agents (CO_2) were introduced to obtain propylene or ethylene single component products. The research group created Ag-Ca-4A for the separation of ethylene and ethane by using Cd^{2+} as a transition metal ion with a similar ion radius to Ca^{2+}

but a greater affinity for olefins [74]. By adding a trace of Cd^{2+} to the 4A zeolite, the pore size rose from 3.95 Å in 4A to 4.05 Å in Cd-A. Furthermore, because Ag^+ has a greater ion radius than Na^+ (1.26 Å vs. 0.95 Å), the low concentration of Ag^+ doping in Cd-A resulted in an enlarged pore size of 4.00 Å in the bimetallic-doped Ag-Cd-4A (as shown in Figure 7b). When combined with DFT computations, Ag^+ causes C_2H_4 molecules to expand, allowing selective access into pore channels with diameters less than 4 Å, resulting in separation effects. As shown in Figure 7c, Ag-Cd-4A has greater Henry selectivity and adsorption capacity than previously reported adsorbents. In terms of kinetic separation, Bereciartua et al. [69] found a flexible pure silica zeolite called ITQ-55 with a heart-shaped cage archi-tecture (as shown in Figure 7d), which has a smaller kinetic diameter than ethylene and ethane and demonstrates strong affinity with ethylene. According to AIMD simulations, the addition of C_2H_4 molecules results in the distortion of the pore windows, which range in size from 2.38 Å to 3.08 Å, leaving only ethylene free to "open" the ITQ-55 pore mouth and speed up diffusion. This method of separation avoids co-adsorption events while displaying the flexibility of the framework and the mechanism of diffusion kinetics. It has important ramifications for ethylene and ethane separation.
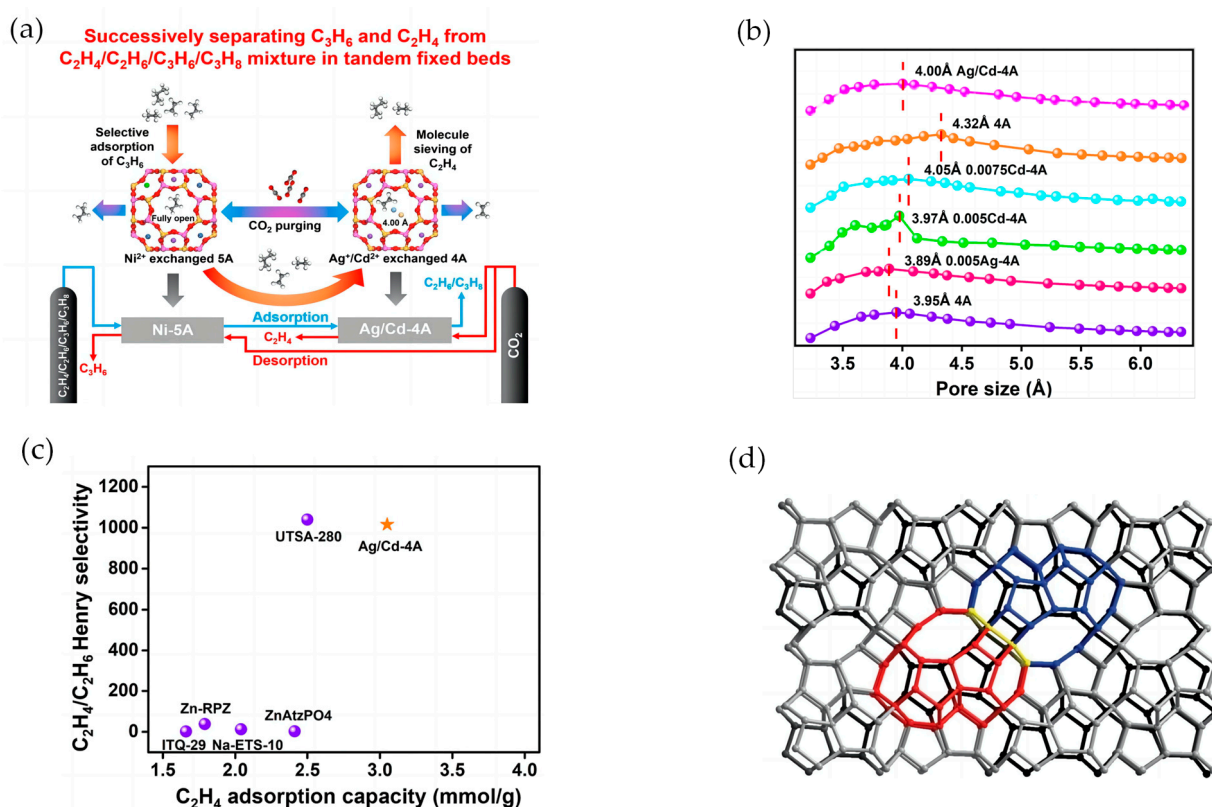
Figure 7. Successively separating C_3H_6 and C_2H_4 from $C_2H_4/C_2H_6/C_3H_6/C_3H_8$ mixture and ITQ-55 cardioid cage topology: (**a**) graphical abstract; (**b**) pore size distributions of 4A, 0.005Ag-4A, 0.05Cd-4A, 0.0075Cd-4A, 0.01Cd-4A, and Ag/Cd-4A.; and (**c**) adsorption capacities and Henry selectivities of C_2H_4 and C_3H_6 on Ag/Cd-4A, and previously reported adsorption materials. Republished from ref. [74], copyright (2023), with permission from Elsevier. (**d**) ITQ-55 cardioid cage topology. Republish from ref. [69], copyright (2017), with permission from AAAS.

### 4.2. Adsorption Separation of Propylene and Propane

One of the five main commodity resins, polypropylene, requires high purity (>99.5%) propylene as its synthesis raw ingredient. Propane, the primary contaminant in the syn-thesis of propylene, has a boiling point that is quite close to that of propylene (just 5.3 K apart) [9]. Traditional low-temperature distillation techniques need a large amount of

energy, which is out of step with the dual-carbon strategy's present trend. Therefore, it is critical to discover an alternate technique that is effective and energy saving.

4.2.1. Metal–Organic Frameworks for Propylene/Propane Separation

　　Pore volume and open metal sites are critical elements influencing MOF separation performance in propylene and propane separation. To improve separation performance, researchers frequently change MOFs from a thermodynamic or kinetic standpoint. The equilibrium-kinetics synergistic method has become a key research focus since Wang et al. [75] reported the high separation performance of Co-MOF-74 in propylene and propane in 2019. Yang et al. [76] created Cu BTC (BTC = benzene-1,3,5-tricarboxylate) by using particular π-Cu bonds to bind strongly with unsaturated metal sites. The C_3H_6/C_3H_8 adsorption selectivity is based on the ultra-microporous structure and can achieve 63.322. Ding et al. [77] reported a phosphoric anion-functionalized metal–organic framework, $ZnAtzPO_4$ (Atz = 3-amino-1,2,4-triazolate), which exhibits a synergistic effect between equilibrium and kinetics for effective separation of propylene and propane (Figure 8a–c). The capture capacity for propylene remains almost unchanged after five cycles, indicating a lower-cost regeneration capability, which is of great significance for industrial applications.
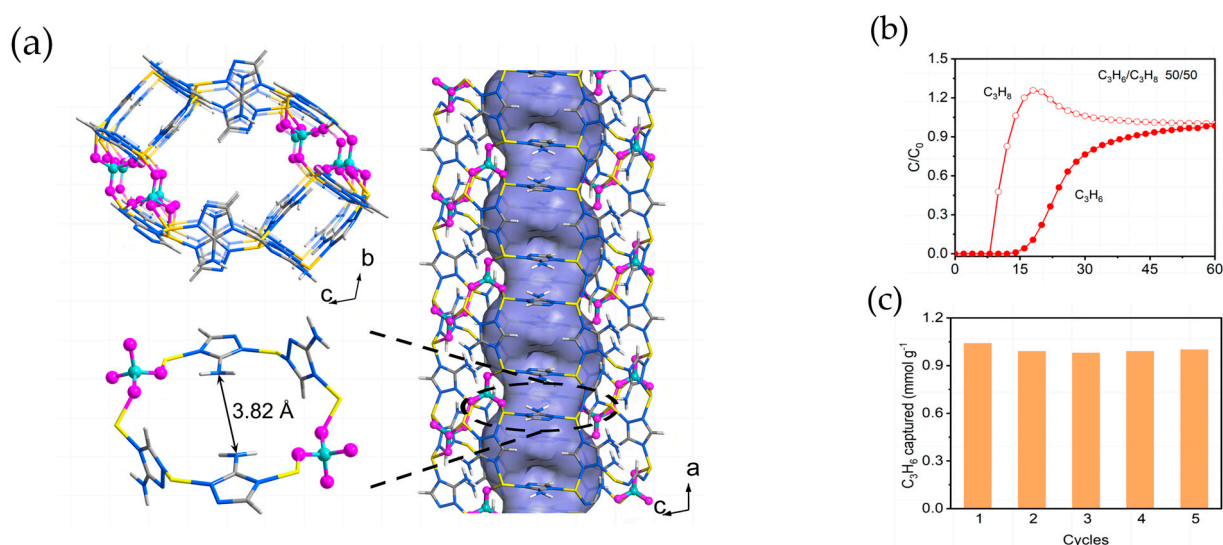

Figure 8. Schematic illustration of the crystal structure of $ZnAtzPO_4$ and penetration curve of molar C_3H_6/C_3H_8 mixture of 298 K and 1.0 bar on $ZnAtzPO_4$: (**a**) local environment and aperture size of the bottleneck-like pore window (Color code: C, gray −40%; H, gray −25%; N, light blue; Zn, yellow; P, aqua; O, pink), (**b**) cyclic breakthrough test of C_3H_6/C_3H_8 (50:50) mixture, and (**c**) five-cycle test experiment. Republish from Ref. [77], Copyright (2020), with permission from Wiley.

　　Furthermore, MOFs with dynamic structures, characterized by unique "molecular gate" effects, have broad prospects for improving the separation selectivity of propylene and propane. These MOF materials can dynamically change their structures from closed non-microporous phases to open porous phases under external stimuli such as temperature and pressure. Zeng et al. [78] suggested a new screening technique (orthogonal array dynamic screening) and created a novel MOF material (JNU-3) based on the dynamic molecular sieve effect. The combination of adsorbent stiffness and dynamic molecular sieve structure, as well as interconnecting dynamic molecular pockets and one-dimensional channels, offers high separation capacity and quick adsorption–desorption kinetics. The adsorption capacity is 58.6 cm^3/g at 1 bar pressure, and the IAST selectivity is 513, greatly above that of similar propylene and propane separation materials. Tan et al. [79] achieved molecule recognition and separation by inserting a temperature-sensitive OMe group into the narrow bottleneck of the ultra-microporous aluminum-based MOF CAU-10. With temperature changes, the effective pore size of the intelligent molecular gate can be continuously adjusted between

3.6 Å and 5.2 Å, covering the size range of commercially important gas molecules. The selectivity for C_3H_6/C_3H_8 reaches 174 at room temperature and pressure.

4.2.2. Molecular Sieves for Propylene/Propane Separation

Zeolites are currently showing promise in the separation of propylene and propane, such as LTA-type [80], FAU-type [81], and CHA-type [82]. Because of their simple and transparent structure, as well as their low cost, LTA-type zeolites have benefits in separation adsorption. Obtaining both high uptake and outstanding separation selectivity, on the other hand, is a prominent research area in the field of propylene and propane separation employing LTA-type zeolites [83,84]. Wang et al. [85] used three-dimensional electron diffraction to study the crystal structure of LTA zeolite with ordered silanols (OSs), as shown in Figure 9a. The findings revealed that OSs were weakly interacting sites with propylene molecules and are related to the zeolite's elliptical eight-membered ring pore structure. This research sheds fresh light on the link between structure and performance at the atomic level, bringing novel insights for the creation of high-performance separation materials. Furthermore, ion exchange and surface chemical modification procedures are useful options for improving the selectivity and adsorption capacity of LTA-type zeolites. Zhou et al. [86] synthesized Ca-Ag-LTA by combining Ag^+ and Ca^{2+} in an LTA-type zeolite. The study demonstrated that precise exchange patterns and metal cation ratios can give zeolites good pore sizes and distinctive recognition sites, resulting in a C_3H_6 uptake of 2.37 mmol/g. Mohammed et al. [87] employed ion exchange to assess the quasi-differential heat of adsorption at 303 K and up to 5 bar for the first time, and used several models to correlate isotherm data to calculate the adsorbent's IAST selectivity for propylene. Figure 9b illustrates the experimental results, and the selectivity of CaNa-LTA for distinguishing propylene/propane IAST is infinitely close to 15 at zero pressure limit. By using methods such as molecular layer deposition (MLD) or atomic layer deposition (ALD), average pore mouth size of 5A zeolite was reduced to be between propane and propylene, therefore, favors propylene separation from propane both thermodynamically and kinetically achieving precise separation. Song et al. [88] created a composite molecular sieve adsorbent by depositing an ultra-thin, porous TiO_2 coating on the outer surface of 5A molecular sieve, which increased the adsorption selectivity of C_3H_6/C_3H_8 substantially. Zhou et al. [89] coated zeolite 5A with n-octadecylphosphonic acid (ODPA), which increased the kinetic selectivity of C3H6/C3H8 substantially over untreated 5A.
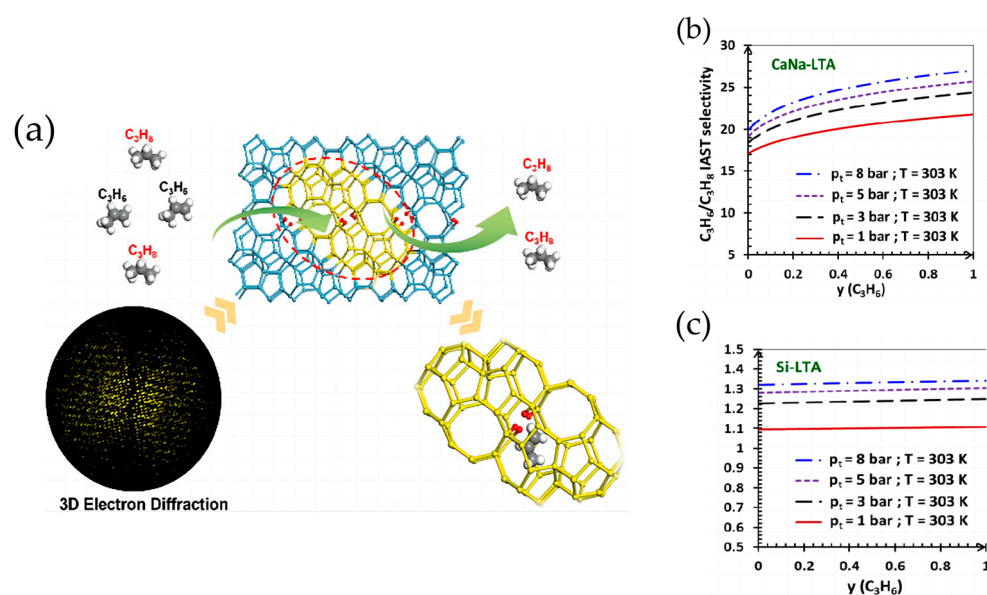
Figure 9. IAST calculation chart of propylene with different adsorbents and structure of ordered silicon hydroxyl pure silicon zeolite under three-dimensional electron diffraction: (**a**) structure of

ordered silicon hydroxyl pure silicon zeolite under three-dimensional electron diffraction. Republished from ref. [85], copyright (2023), with permission from ACS; (**b**) IAST calculations for the adsorption, on MgNa-LTA and (**c**) IAST calculations for the adsorption, on Si-LTA. Republished from ref. [87], copyright (2022), with permission from Elsevier.

5. Adsorptive Separation of Isomers in High-Carbon Hydrocarbons (C₆–C₈) Using Metal–Organic Frameworks and Molecular Sieves

Adsorption separation of low-carbon hydrocarbons (C₁–C₃) utilizing metal–organic frameworks and molecular sieves has made significant progress. The separation of C₆–C₈ hydrocarbon isomers, on the other hand, is still in its early stages of investigation. High-carbon hydrocarbons have various isomers, unlike low-carbon hydrocarbons; one current research focus in the field of high-carbon hydrocarbon separation is the recovery of isomers from straight-chain alkanes to suit market demands [90]. C₆ (hexane), in particular, holds a key place in the petrochemical sector as a basic raw material in the gasoline industry. The presence of up to five isomers of C₆ hydrocarbons limits the petrochemical industry's future expansion to some extent [91]. Based on three methods of separation that have been thoroughly researched, research has revealed that metal–organic frameworks and molecular sieves can efficiently separate straight-chain alkanes. Furthermore, studying the adsorptive separation systems of high-carbon hydrocarbon isomers can help to improve the material systems for hydrocarbon adsorptive separation, allowing for the prediction and control of adsorbent separation performance and the attainment of optimal separation effects.

5.1. Metal–Organic Frameworks for High-Carbon Hydrocarbons (C₆–C₈) Isomer Separation

In contrast to kinetic and thermodynamic equilibrium effects, the sieving effect of molecular sieves is a low-energy and highly selective method for efficiently separating linear, mono-branched, and di-branched hexane isomers utilizing metal–organic frameworks. Metal–organic frameworks can tailor pore volume, pore size, and other pore architectures via mixed ligand pore engineering by changing connections or ligands, resulting in efficient separation of gas molecules with greater kinetic diameters [92]. Yu et al. [93] used a mixed ligand method to create two novel CAU-10 series MOFs, CAU-10-H, and CAU-10-Br. These MOFs may tolerate n-hexane (n-Hex) and 3-methylpentane (3-MP) while rejecting 2,2-dimethylbutane (2,2-DMB) by ligand replacement and precision mixing, allowing for successful separation of mono-branched and di-branched hexane isomers. Guo et al. [94] designed a unique HIAM-410LI material with an FTW network using 12 Zr₆ nodes and 4 tetracarboxylate linkers on HIAM-410. This MOF not only has high hydrothermal stability, but also enables pore structure customization for perfect separation of mono-branched and di-branched hexane isomers. Unlike Guo et al., Bhajan et al. [95] expanded the dimensionality of the connectors from 2D to 3D to adjust pore size with sub-angstrom precision, reducing the likelihood of low separating efficiency. due to connector rotation. By hybridizing two organic ligands, 2-methylimidazole (2-MeIM) and formaldehyde-2-methylimidazole (OHC-IM), into the metal–organic framework ZIFs, our team [96] successfully created a series of hybrid connector ZIF-8-90 samples (as shown in Figure 10).

### 5.2. Molecular Sieves for High-Carbon Hydrocarbons (C₆–C₈) Isomer Separation

In the petrochemical sector, 5A molecular sieves are frequently used as adsorbent materials for the separation of isomers of high-carbon hydrocarbons, especially for the isolation of n-alkanes from hydrocarbon mixtures [97]. Conventional approaches for creating 5A molecular sieves, however, have poor separation and diffusion performance. In light of this, Liu et al. [98] used TPOAC as a template to create a variety of multi-level porous molecular sieves containing micropores and mesopores. The diffusion rate of high-carbon n-alkanes (pentane and hexane) in these molecular sieves has increased by an order of magnitude in comparison to 5A molecular sieves made using standard

techniques, according to experimental results, making it easier to separate them from isomers. Furthermore, a binder must be added during the synthesis process to provide the molecular sieve the requisite mechanical strength. However, the performance of adsorption can be adversely affected by the presence of a binder to some extent. Thus, through in-situ hydrothermal modification of premade silica gel precursors, our team created binder-free 5A molecular sieves (as depicted in Figure 11). Following comparisons with 5A molecular sieves that contain a binder, its saturation adsorption capacity for n-alkanes increased by 25% to 35%, breakthrough adsorption quantity increased by 115% to 130%, and the mass transfer zone's length was greatly decreased [99,100]. Although molecular sieve materials have intrinsic stiffness limitations, little diversity, and less attractive adsorption performance improvement opportunities than MOFs, they are extensively utilized in industry due to their reliable hydrothermal performance and affordable price.
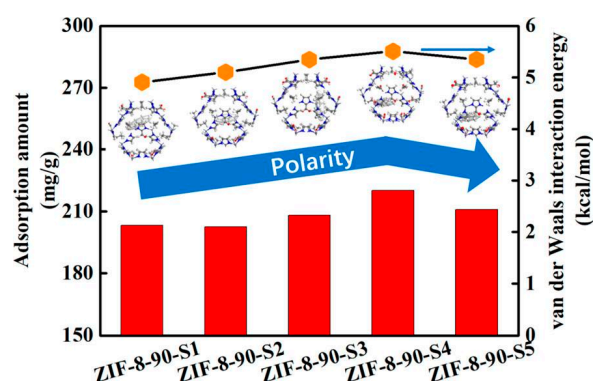
Figure 10. Structural schematic diagram of ZIF-8-90. Republished from ref. [96], copyright (2023), with permission from ACS.
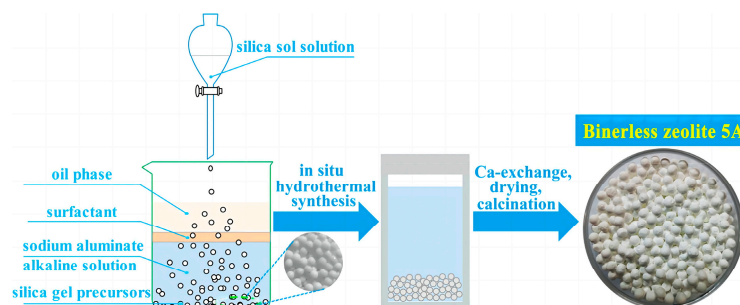
Figure 11. Schematic diagram of unbonded 5A zeolite synthesis. Republished from ref. [99], copyright (2019), with permission from ACS.

6. Perspectives

6.1. Challenges

(1) Several effective adsorption separation materials have been created recently, although they have only been used in lab settings. Even if their hydrothermal stability is still subpar, their separation performance will be significantly compromised in humid and hot application scenarios. Furthermore, the use of organic solvents and precious metals for modification raises the cost of adsorbents, posing small environmental hazards. This makes large-scale manufacturing difficult. The research on the concept of carbon neutrality and the study on recyclability during the gas adsorption process still have certain gaps, nevertheless.

(2) Even when achieving large adsorption capacity or high separation selectivity, it is currently not possible to accomplish both huge adsorption capacity and high separation selectivity in carbon hydrocarbon compounds separation and purification. More in-depth research should be performed on the transport mechanism and sepa-

ration performance of molecules in MOFs and molecular sieves in order to improve material design, increase separation efficiency, design adsorbents with both a large adsorption capacity and high selectivity, and achieve more effective, energy-saving, and environmentally friendly low-carbon hydrocarbon separation.

6.2. Opportunities

(1) Hierarchical combination design of different adsorbent materials

Currently, the majority of adsorbent materials are carbon and crystal materials, albeit separation performance is typically subpar and much of their research is focused on single separation scenarios. However, if we can combine different adsorbent material types into a single material at a time to generate multifunctional adsorbent materials, the separation performance might surprise improve. Furthermore, the drawbacks of a single adsorbent loading can be improved by carefully combining MOFs or molecular sieves with different functionalities on a single fixed bed.

(2) Computer-aided data processing and simulation for screening adsorbents

Technology advancements today make it possible to build enormous computer databases with tens of thousands of distinct adsorbents, faithfully recreating their microstructure, including their pore size, structure, and other features. When employing big data analysis to further screen and foresee suitable adsorbent materials, the performance of adsorption separation may be enhanced by creatively combining the structure–effect link with theoretical calculations.

7. Conclusions

An eco-friendly, low-carbon economy has emerged as the main trend for future development under the current "carbon neutrality" policy. One of the essential processes for the petrochemical industry's sustainable development and a major route to a low-carbon economy is the effective separation and purification of carbon hydrocarbon compounds. Adsorption separation is a cutting-edge technique for separating low-carbon hydrocarbons, and its benefits of low investment, low energy use, and high efficiency play a vital part in this process as well as in the transformation of the energy structure. This article discusses the most recent scientific advances in separation and purification of carbon hydrocarbon compounds utilizing two of the most prominent adsorbent materials, metal–organic frameworks and molecular sieves. And combine existing separation mechanisms (thermodynamic equilibrium effect, molecular sieve effect, and kinetic effect) to investigate the relationship between structural composition and properties, as well as separation performance and mechanism, in order to provide reference opinions for the design of new adsorption materials. We believe that with interdisciplinary collaboration, the separation performance of carbon hydrocarbon compounds can be improved in the near future.

Author Contributions: Conceptualization, H.S.; methodology, Y.Z. and Y.W.; writing—original draft preparation, Y.Z.; data curation, Y.Z. and P.L.; and writing—review and editing, Y.Z., P.L., Q.Z. and H.S. All authors have read and agreed to the published version of the manuscript.

Institutional Review Board Statement: Not applicable.

Informed Consent Statement: Not applicable.

Data Availability Statement: Not applicable.

Conflicts of Interest: The authors declare no conflict of interest.

References

1. Frank, D.M. The light hydrocarbons in petroleum: A critical review. *Org. Geochem.* **1997**, *26*, 417–440. [CrossRef]
2. Chen, X.Y.; Xiao, A.; Rodrigue, D. Polymer-based Membranes for Propylene/Propane Separation. *Sep. Purif. Rev.* **2021**, *51*, 130–142. [CrossRef]
3. Zhang, Q.; Lian, X.; Rajamani, K.; Yang, S.; Hu, T. An ultramicroporous metal-organic framework based on octahedral-like cages showing high-selective methane purification from a six-component $C_1/C_2/C_3$ hydrocarbons mixture. *Sep. Purif. Rev.* **2023**, *304*, 122312. [CrossRef]
4. Shi, R.F.; Lv, D.F.; Chen, Y.W.; Wu, H.X.; Liu, B.Y.; Xia, Q.B.; Li, Z. Highly selective adsorption separation of light hydrocarbons with a porphyrinic zirconium metal-organic framework PCN-224. *Sep. Purif. Rev.* **2023**, *207*, 262–268. [CrossRef]
5. Jiang, Y.J.; Hu, Y.Q.; Luan, B.Q.; Wang, L.Y.; Krishna, R.; Ni, H.F.; Hu, X.; Zhang, Y.B. Benchmark single-step ethylene purification from ternary mixtures by a customized fluorinated anion-embedded MOF. *Nat. Commun.* **2023**, *14*, 401. [CrossRef]
6. Jiang, H.F.; Chen, Y.; Song, S.Q.; Guo, Z.Y.; Zhang, Z.Q.; Zheng, C.Y.; He, G.W.; Wang, H.J.; Wu, H.; Huang, T.; et al. Confined facilitated transport within covalent organic frameworks for propylene/propane membrane separation. *Chem. Eng. J.* **2022**, *439*, 135657. [CrossRef]
7. Park, H.M.; Lee, J.Y.; Jee, K.Y.; Nakao, S.; Lee, Y.T. Hydrocarbon separation properties of a CVD-deposited ceramic membrane under single gases and binary mixed gas. *Sep. Purif. Rev.* **2021**, *254*, 117642–117651. [CrossRef]
8. Lee, J.; Chuah, C.Y.; Kim, J.; Kim, Y.; Nakeun, K.; Seo, Y.; Kim, K.; Bae, T.H. Separation of acetylene from carbon dioxide and ethylene by a water-stable microporous metal–organic framework with aligned imidazolium groups inside the channels. *Angew. Chem. Int. Ed.* **2018**, *130*, 7995–7999. [CrossRef]
9. Cui, X.L.; Xing, H.B. Research progress on separation of low-carbon hydrocarbons from metal-organic framework materials. *CIESC J.* **2018**, *69*, 2339–2352. [CrossRef]
10. Sholl, D.S.; Lively, R.P. Seven chemical separations to change the world. *Nature* **2016**, *532*, 435–437. [CrossRef]
11. Yang, L.F.; Qian, S.H.; Wang, X.B.; Cui, X.L.; Chen, B.L.; Xing, H.B. Energy-efficient separation alternatives: Metal–organic frameworks and membranes for hydrocarbon separation. *Chem. Soc. Rev.* **2020**, *49*, 5359–5406. [CrossRef]
12. Wu, N.; Xue, H. Comparative study on shallow cooling process of light hydrocarbon recovery from associated gas in oilfield. *Chem. Eng. Des. Commun.* **2020**, *30*, 6–11. [CrossRef]
13. Chuah, C.Y.; Bae, T.H. Recent advances in mixed-matrix membranes for light hydrocarbon (C_1–C_3) separation. *Membranes* **2022**, *12*, 201. [CrossRef]
14. Lively, R.P.; Sholl, D.S. From water to organics in membrane separations. *Nat. Mater.* **2017**, *16*, 276–279. [CrossRef]
15. Ko, D. Optimization of vacuum pressure swing adsorption processes to sequester carbon dioxide from coalbed methane. *Ind. Eng. Chem. Res.* **2016**, *55*, 8967–8978. [CrossRef]
16. Zhai, R.; Jiao, F.L.; Lin, H.J.; Hao, F.R.; Li, J.B.; Yan, H.; Li, N.N.; Wang, H.H.; Jin, Z.Y.; Zhang, Y.J.; et al. Research progress of metal-organic framework materials. *Chin. J. Chromatogr.* **2014**, *32*, 107–116. [CrossRef]
17. Wang, Y.S.; Zhang, X.J.; Ba, Y.Q.; Li, T.Y.; Hao, G.P.; Lu, A.H. Recent advances in carbon-based adsorbents for adsorptive separation of light hydrocarbons. *Research* **2022**, *2022*, 9780864. [CrossRef]
18. Qin, Y.; Gao, X.; Zhang, H.T.; Zhang, S.H.; Zheng, L.G.; Li, Q.; Mo, Z.S.; Duan, L.H.; Zhang, X.T.; Song, L.J. Measurements and distinguishment of mass transfer processes in fluid catalytic cracking catalyst particles by uptake and frequency response methods. *Catal. Today* **2015**, *245*, 147–154. [CrossRef]
19. He, Y.; Xiang, S.C.; Chen, B.L. A microporous hydrogen-bonded organic framework for highly selective C_2H_2/C_2H_4 separation at ambient temperature. *J. Am. Chem. Soc.* **2011**, *133*, 14570–14573. [CrossRef]
20. Lin, R.; Wu, H.; Li, L.B.; Tang, X.; Li, Z.Q.; Gao, J.K.; Cui, H.; Zhou, W.; Chen, B.L. Boosting ethane/ethylene separation within isoreticular ultramicroporous metal-organic frameworks. *J. Am. Chem. Soc.* **2018**, *140*, 2940–12946. [CrossRef]
21. Li, L.B.; Lin, R.; Wang, X.Q.; Zhou, W.; Jia, L.T.; Li, J.P.; Chen, B.L. Kinetic Separation of Propylene over Propane in a Microporous Metal-Organic Framework. *Chem. Eng. J.* **2018**, *354*, 977–982. [CrossRef]
22. Xu, S.; Liu, R.S.; Zhang, M.Y.; Lu, A. Designed synthesis of porous carbons for the separation of light hydrocarbons. *Chin. J. Chem. Eng.* **2022**, *42*, 130–150. [CrossRef]
23. Hao, X.F. Preparation of Modified Clinoptilolite Zeolite and Its CH_4/N_2 Adsorption and Separation Performance. Ph.D. Thesis, China University of Geosciences, Beijing, China, 2020.
24. Liu, J.Q. Synthesis of Nanozeolite and Study on the Adsorption and Separation Performance of CH_4/N_2. Ph.D. Thesis, Taiyuan University of Technology, Taiyuan, China, 2021.
25. Freitas, M.; Figueiredo, J. Preparation of carbon molecular sieves for gas separations by modification of the pore sizes of activated carbons. *Fuel* **2001**, *80*, 1–6. [CrossRef]
26. Smit, B.; Maesen, T.L.M. Towards a molecular understanding of shape selectivity. *Nature* **2008**, *451*, 671–678. [CrossRef]
27. Zhang, W.C.; Cheng, Y.H.; Guo, C.S.; Xie, C.P. Cobalt Incorporated Porous Aromatic Framework for CO_2/CH_4 Separation. *Ind. Eng. Chem. Res.* **2018**, *57*, 10985–10991. [CrossRef]
28. Guo, P.; Li, M. Research Progress on CH_4/N_2 Separation Process in Coal-bed Methane. *Chem. Ind. Eng. Prog.* **2008**, *7*, 963. [CrossRef]
29. He, Y.B.; Zhou, W.; Qian, G.D.; Chen, B.L. Methane storage in metal-organic frameworks. *Chem. Soc. Rev.* **2014**, *43*, 5657–5678. [CrossRef]

30. Niu, Z.; Cui, X.L.; Pham, T.; Lan, P.C.; Xing, H.B.; Forrest, K.A.; Wojtas, L.; Space, B.; Ma, S.Q. A Metal-Organic Framework Based Methane Nano-trap for the Capture of Coal-Mine Methane. *Angew. Chem. Int. Ed.* **2019**, *58*, 10138–10141. [CrossRef]

31. Chang, M.; Ren, J.H.; Yang, Q.Y.; Liu, D.H. A robust calcium-based microporous metal-organic framework for efficient CH_4/N_2 separation. *Chem. Eng. J.* **2021**, *408*, 127294–127301. [CrossRef]

32. Chang, M.; Yan, T.G.; Wei, Y.; Wang, J.X.; Liu, D.H.; Chen, J.F. Enhancing CH_4 Capture from Coalbed Methane through Tuning van der Waals Affinity within Isoreticular Al-Based Metal-Organic Frameworks. *ACS Appl. Mater. Interfaces* **2022**, *14*, 25374–25384. [CrossRef]

33. Wang, S.M.; Shivanna, M.; Yang, Q.Y. Nickel-Based Metal-Organic Frameworks for Coal-Bed Methane Purification with Record CH_4/N_2 Selectivity. *Angew. Chem. Int. Ed.* **2022**, *61*, 202201017–202201024. [CrossRef]

34. Li, T.; Jia, X.X.; Cheng, H.; Chang, Z.Y.; Li, L.B.; Wang, Y.; Li, J.P. Tuning the Pore Environment of MOFs toward Efficient CH_4/N_2 Separation under Humid Conditions. *ACS Appl. Mater. Interfaces* **2022**, *14*, 15830–15839. [CrossRef] [PubMed]

35. Wang, X.H. Synthesis and Modification of SAPO Molecular Sieve and Its Separation Performance for Small Molecules. Ph.D. Thesis, Jilin University, Changchun, China, 2021.

36. Yang, J.F.; Zhao, Q.; Xu, H. Adsorption of CO_2, CH_4 and N_2 on Gas Diameter Grade Ion-Exchange Small Pore Zeolites. *J. Chem. Eng. Data* **2012**, *57*, 3701–3709. [CrossRef]

37. Yang, J.F.; Liu, J.Q.; Liu, P.X.; Li, L.B.; Tang, X.; Shang, H.; Li, J.P.; Chen, B.L. K-Chabazite Zeolite Nanocrystal Aggregates for Highly Efficient Methane Separation. *Angew. Chem. Int. Ed.* **2021**, *61*, 202116850–202116856. [CrossRef]

38. Chen, Y.H.; Peng, Q.L.; Jiang, H.; Sun, H.; Shen, B.X.; Zhang, J.; Li, W.L.; Liu, Y.J.; Guo, L. Sr^{2+} exchange regulates the selective adsorption of N_2 in CH_4 by ETS-4 zeolite. *Acta Pet. Sin. Pet. Process. Sect.* **2022**, *38*, 1–10. [CrossRef]

39. Feng, Y.Y.; Yang, W.; Wang, N.; Chu, W.; Liu, D.J. Effect of nitrogen-containing groups on methane adsorption behaviors of carbon spheres. *J. Anal. Appl. Pyrolysis* **2014**, *107*, 204–210. [CrossRef]

40. Yang, Z.Y.; Wang, D.C.; Meng, Z.Y.; Li, Y.Y. Adsorption separation of CH_4/N_2 on modified coal-based carbon molecular sieve. *Sep. Purif. Rev.* **2019**, *218*, 1505–1511. [CrossRef]

41. Zhang, J.H.; Qu, S.D.; Li, L.T.; Wang, P.; Li, X.F.; Che, Y.F.; Li, X.L. Preparation of Carbon Molecular Sieves Used for CH_4/N_2 Separation. *J. Chem. Eng. Data* **2018**, *63*, 1737–1744. [CrossRef]

42. Toledo-cervantes, A.; Estrada, J.; Lebrero, R.; Raul, M. A comparative analysis of biogas upgrading technologies: Photosynthetic vs. physical/chemical processes. *Algal Res.* **2017**, *25*, 237–243. [CrossRef]

43. Zhang, S.Y.; Liu, H.; Liu, P.F.; Wu, P.P.; Yang, Z.H.; Yang, Q.Y.; Liu, X.H. Research Progress of Metal-Organic Framework Materials in CO_2/CH_4 Adsorption and Separation. *CIESC J.* **2014**, *65*, 1563–1570. [CrossRef]

44. Li, J.R.; Kuppler, R.J.; Zhou, H.C. Selective Gas Adsorption Separation in Metal-Organic Frameworks. *Chem. Soc. Rev.* **2009**, *38*, 1477–1504. [CrossRef] [PubMed]

45. Alvarez, N.; Gil, M.V.; Rubiera, F.; Pevida, C. Adsorption performance indicators for the CO_2/CH_4 separation: Application to biomass-based activated carbons. *Fuel Process. Technol.* **2016**, *142*, 361–369. [CrossRef]

46. Yuan, S.; Feng, L.; Wang, K.C.; Pang, J.D.; Bosch, M.; Lollar, C.; Sun, Y.J.; Qin, J.S.; Yang, X.Y.; Zhang, P.; et al. Stable Metal-Organic Frameworks: Design, Synthesis, and Applications. *Adv. Mater.* **2018**, *30*, 1704303. [CrossRef] [PubMed]

47. Cui, W.G.; Hu, T.L.; Bu, X.H. Metal–Organic Framework Materials for the Separation and Purification of Light Hydrocarbons. *Adv. Mater.* **2020**, *32*, 1806445. [CrossRef] [PubMed]

48. Chen, S.J.; Li, X.J.; Duan, J.; Fu, Y.; Wang, Z.Y.; Zhu, M.; Li, N. Investigation of highly efficient adsorbent based on Ni-MOF-74 in the separation of CO_2 from natural gas. *Chem. Eng. J.* **2021**, *419*, 129653–129662. [CrossRef]

49. Zhang, J.W.; Qu, P.; Hu, M.C.; Li, S.N.; Jiang, Y.C.; Zhai, Q.G. Self-Assembly of a Rare Nanocage-based Fe-MOF toward High Methane Purification Performance. *Cryst. Growth Des.* **2020**, *20*, 5657–5663. [CrossRef]

50. Zheng, B.S.; Luo, X.; Wang, Z.X.; Zhang, S.W.; Yun, R.R.; Huang, L.; Zeng, W.J.; Liu, W.L. An unprecedented water stable acylamide-functionalized metal-organic framework for highly efficient CH_4/CO_2 gas storage/separation and acid–base cooperative catalytic activity. *Inorg. Chem. Front.* **2018**, *5*, 2355–2363. [CrossRef]

51. Ko, D. Comparison of carbon molecular sieve and zeolite 5A for CO_2 sequestration from CH_4/CO_2 mixture gas using vacuum pressure swing adsorption. *Korean J. Chem. Eng.* **2021**, *38*, 1043–1051. [CrossRef]

52. Yang, H.; Li, W.; Gao, H. Purification of CH_4 from CH_4/CO_2 mixture using carbon-based adsorbents. *Trans. Chin. Soc. Agric. Mach.* **2013**, *44*, 154–157. [CrossRef]

53. Lei, L.F.; Bai, L.; Lindbråthen, A.; Pan, F.J.; Zhang, X.P.; He, X.Z. Carbon membranes for CO_2 removal: Status and perspectives from materials to processes. *Chem. Eng. J.* **2020**, *401*, 126084. [CrossRef]

54. Liang, J.P.; Ma, B.W. Preparation of Coconut Shell Activated Carbon for CH_4/CO_2 Separation in Coalbed Methane. *Chieh Ching Mei Chi Shu* **2021**, *27*, 254–261. [CrossRef]

55. Kaya, M.; Atelge, M.R.; Bekirogullari, M.; Eskicioglu, C.; Atabani, A.E.; Kumar, G.L.; Yildiz, Y.S.; Unalan, S. Carbon molecular sieve production from defatted spent coffee ground using $ZnCl_2$ and benzene for gas purification. *Fuel* **2020**, *277*, 118183–118194. [CrossRef]

56. Orlando, F.C.; Ignacio, C.G.; Manuel, M.E.; Carlos, R.R.; Joaquín, S.A. Activated carbon from polyurethane residues as molecular sieves for kinetic adsorption/separation of CO_2/CH_4. *Colloids Surf.* **2022**, *652*, 129882–129887.

57. Wang, Y.X.; Shing, B.P.; Zhao, D. Alternatives to Cryogenic Distillation: Advanced Porous Materials in Adsorptive Light Olefin/Paraffin Separations. *Small* **2019**, *15*, 1900058–1900096. [CrossRef]

58. Wu, H.X. Synthesis of Several Microporous MOFs and Their Adsorption Separation for C_2H_4/C_2H_6 and C_3H_6/C_3H_8. Ph.D. Thesis, South China University of Technology, Guangzhou, China, 2021.

59. Wu, C.H.; Zhang, K.X.; Wang, H.L.; Fan, Y.Q.; Zhang, S.W.; He, S.F.; Wang, F.; Tao, Y.; Zhao, X.W.; Zhang, Y.B.; et al. Enhancing the Gas Separation Selectivity of Mixed-Matrix Membranes Using a Dual-Interfacial Engineering Approach. *J. Am. Chem. Soc.* **2022**, *14*, 18503–18512. [CrossRef]

60. Suo, C.; Ma, J.; Zhao, N.; Wang, R.C.; Zhu, R.Z.; Wang, L.; He, J.X. Research on carbon peaking and carbon neutrality path of chemical enterprises. *China Rubber* **2022**, *48*, 14–20. [CrossRef]

61. Yu, J.J.; Zhang, X.; Wu, X.X.; Liu, T.; Zhang, Z.Q.; Wu, J.; Zhu, C. Metal-free radical difunctionalization of ethylene. *Chem* **2023**, *9*, 472–482. [CrossRef]

62. Lv, D.F.; Zhou, P.J.; Xu, J.H.; Tu, S.; Xu, F.; Yan, J.; Xi, H.X.; Yuan, W.B.; Fu, Q.; Chen, X.; et al. Recent advances in adsorptive separation of ethane and ethylene by C_2H_6-selective MOFs and other adsorbents. *Chem. Eng. J.* **2022**, *431*, 133208. [CrossRef]

63. Gao, F.; Wang, Y.Q.; Wang, X. Ethylene/ethane separation by CuCl/AC adsorbent prepared using $CuCl_2$ as a precursor. *Adsorption* **2016**, *22*, 1013–1022. [CrossRef]

64. Chang, G.G.; Huang, M.H.; Su, Y.; Xing, H.B.; Su, B.Z.; Zhang, Z.G.; Yang, Q.W.; Yang, Y.W.; Ren, Q.L.; Bao, Z.B.; et al. Immobilization of Ag(i) into a metal-organic framework with -SO_3H sites for highly selective olefin-paraffin separation at room temperature. *Chem. Commun.* **2015**, *51*, 2859–2862. [CrossRef]

65. Yin, Y.; Zhang, Z.Z.; Xu, C.L.; Wu, H.; Shi, L.; Wang, S.J.; Xu, X.Y.; Yuan, A.H.; Wang, S.B.; Sun, H.Q. Confinement of Ag(I) Sites within MIL-101 for Robust Ethylene/Ethane Separation. *ACS Sustain. Chem. Eng.* **2019**, *8*, 823–830. [CrossRef]

66. Bao, Z.B.; Wang, J.W.; Zhang, Z.G.; Xing, H.B.; Yang, Q.W.; Yang, Y.W.; Wu, H.; Krishna, R.; Zhou, W.; Chen, B.L.; et al. Molecular Sieving of Ethane from Ethylene through the Molecular Cross-Section Size Differentiation in Gallate-Based Metal-Organic Frameworks. *Angew. Chem. Int. Ed.* **2018**, *57*, 16020–16025. [CrossRef]

67. Zeng, H.; Xie, X.J.; Xie, M.; Huang, Y.L.; Luo, D.; Wang, T.; Zhao, Y.F.; Lu, W.G.; Li, D. Cage-Interconnected Metal-Organic Framework with Tailored Apertures for Efficient C_2H_6/C_2H_4 Separation under Humid Conditions. *AICHE J.* **2019**, *141*, 20390–20396. [CrossRef] [PubMed]

68. Liu, Y.Z.; Wu, Y.; Liang, W.W.; Peng, J.J.; Li, H.; Wang, H.H.; Janik, M.; Xiao, J. Bimetallic ions regulate pore size and chemistry of zeolites for selective adsorption of ethylene from ethane. *Chem. Eng. Sci.* **2020**, *220*, 115636–115648. [CrossRef]

69. Bereciartua, P.; Cantin, A.; Corma, A.; Jorda, J.L.; Palomino, M.; Rey, F.; Valencia, S.; Corcoran, E.W., Jr.; Kortunov, P.; Casty, G.L. Control of zeolite framework flexibility and pore topology for separation of ethane and ethylene. *Science* **2017**, *358*, 1068–1071. [CrossRef] [PubMed]

70. Di, Z.Y.; Liu, C.P.; Pang, J.D.; Zou, S.X.; Ji, Z.Y.; Hu, F.L.; Chen, C.; Yuan, D.Q.; Hong, M.C.; Wu, M.Y. A Metal-Organic Framework with Nonpolar Pore Surfaces forthe One-Step Acquisition of C_2H_4 from a C_2H_4 and C_2H_6 Mixture. *Angew. Chem. Int. Ed.* **2022**, *61*, e202210343. [CrossRef] [PubMed]

71. Bian, Q.M.; Xin, M.D.; Zou, K.; Xu, G.T. Research Progress of Molecular Sieve and Metal-Organic Framework Materials for Ethylene/Ethane Separation. *Acta Pet. Sin. Pet. Process. Sect.* **2020**, *36*, 866–877. [CrossRef]

72. Wang, Q.X. Design, Preparation and Gas Separation Performance Evaluation of Carbon Molecular Sieve Membranes. Master's Thesis, China University of Petroleum, Beijing, China, 2020.

73. Zandvoort, I.V.; Klink, G.V.; Jong, E.; Waal, J. Selectivity and stability of zeolites [Ca]A and [Ag]A towards ethylene adsorption and desorption from complex gas mixtures. *Microporous Mesoporous Mater.* **2018**, *263*, 142–149. [CrossRef]

74. Chen, Y.; Jiang, H.; Peng, Q.L.; Fang, D.Y.; Liu, C.L.; Wu, K.G.; Chen, Y.X.; Gao, W.K.; Wang, H.; Yang, F.J.; et al. Successively separating C_3H_6 and C_2H_4 from $C_2H_4/C_2H_6/C_3H_6/C_3H_8$ mixture in tandem fixed beds involving two zeolites LTA well-regulated via low transition-metal doping. *Chem. Eng. J.* **2023**, *47*, 145151. [CrossRef]

75. Wang, Y.; Huang, N.Y.; Zhang, X.W.; He, H.; Huang, R.K.; Ye, Z.M.; Li, Y.; Zhou, D.D.; Liao, P.Q.; Chen, X.M.; et al. Selective Aerobic Oxidation of a Metal-Organic Framework Boosts Thermodynamic and Kinetic Propylene/Propane Selectivity. *Angew. Chem. Int. Ed.* **2019**, *58*, 7692–7696. [CrossRef]

76. Yang, P.; Meng, X.H.; Guo, P.H.; Zhou, R.J.; Zhang, Y.H.; Cao, S.; Zhang, D.; Ji, H.B.; Duan, L.H. Highly selective separation of C_3H_6/C_3H_8 within hierarchical metal–organic CuxOy@HP–Cu–BTCs. *Mater. Chem. Phys.* **2023**, *294*, 127024–127037. [CrossRef]

77. Ding, Q.; Zhang, Z.Q.; Yu, C.; Zhang, P.X.; Wang, J.; Kong, L.Y.; Cui, X.L.; He, C.H.; Deng, S.G.; Xing, H.B. Separation of propylene and propane with a microporous metal-organic framework via equilibrium-kinetic synergetic effect. *AICHE J.* **2020**, *67*, 17094–17102. [CrossRef]

78. Zeng, H.; Xie, M.; Wang, T.; Wei, R.J.; Xie, X.J.; Zhao, Y.F.; Lu, W.G.; Li, D. Orthogonal-array dynamic molecular sieving of propylene/propane mixtures. *Nature* **2021**, *595*, 542–548. [CrossRef] [PubMed]

79. Tan, Q.; Huang, H.L.; Peng, Y.G.; Chang, Y.J.; Zhang, Z.; Liu, D.H.; Zhong, C.L. A temperature-responsive smart molecular gate in a metal–organic framework for task-specific gas separation. *J. Mater. Chem. A* **2019**, *7*, 26574–26579. [CrossRef]

80. Zhang, Y.P.; Zhang, S.Z.; Wang, H.T.; Zhang, Y. Research Progress on Acrylic/Propane Adsorption and Separation Materials. *Fine Chem.* **2020**, *37*, 1327–1333. [CrossRef]

81. Moradi, H.; Azizpour, H.; Bahmanyar, H.; Emamian, H. Emamian Molecular dynamic simulation of carbon dioxide, methane, and nitrogen adsorption on Faujasite zeolite. *Chin. J. Chem. Eng.* **2022**, *43*, 70–76. [CrossRef]

82. Olson, D.; Camblor, M.; Villaescusa, L.; Kuehl, G.H. Light hydrocarbon sorption properties of pure silica Si-CHA and ITQ-3 and high silica ZSM-58. *Microporous Mesoporous Mater.* **2003**, *67*, 27–33. [CrossRef]

83. Fu, D.L.; Park, Y.; Davis, M.E. Zinc containing small-pore zeolites for capture of low concentration carbon dioxide. *Angew. Chem. Int. Ed.* **2021**, *134*, 2–9. [CrossRef]

84. Xiong, Y.; Woodward, R.T.; Danaci, D.; Evans, A.; Tian, T.; Azzan, H.; Ardakani, M.; Petit, C. Understanding trade-offs in adsorption capacity, selectivity and kinetics for propylene/propane separation using composites of activated carbon and hypercrosslinked polymer. *Chem. Eng. J.* **2021**, *426*, 131628–131636. [CrossRef]

85. Wang, J.; Ma, C.; Liu, J.Q.; Liu, Y.; Xu, X.Q.; Xie, M.; Wang, H.; Wang, L.; Guo, P.; Liu, Z.M. Pure Silica with Ordered Silanols for Propylene/Propane Adsorptive Separation Unraveled by Three-Dimensional Electron Diffraction. *AICHE J.* **2023**, *145*, 6853–6860. [CrossRef]

86. Zhou, X.Y.; Miao, G.; Xu, G.D.; Luo, J.Z.; Yang, C.T.; Xiao, J. Mixed (Ag^+, Ca^{2+})-LTA zeolite with suitable pore feature for effective separation of C_3H_6/C_3H_8. *Chem. Eng. J.* **2022**, *45*, 137913–137923. [CrossRef]

87. Benchaabane, M.A.; Goncalves, G.T.; Bloch, E.; Palllaudean, J.L.; Daou, T.J.; Bourrelly, S.; Chaplais, G.; Llewellyn, P.L. An initial evaluation of the thermodynamic or kinetic separation performance of cation-exchanged LTA zeolites for mixtures of propane and propylene. *Microporous Mesoporous Mater.* **2022**, *344*, 112211–112227. [CrossRef]

88. Song, Z.N.; Huang, Y.; Wang, L.; Li, S.G.; Yu, M. Composite 5A zeolite with ultrathin porous TiO_2 coating for selective gas adsorption. *Chem. Commun.* **2015**, *51*, 373–375. [CrossRef]

89. Zhou, X.P.; Falconer, J.L.; Medlin, J.W. Mechanism of selectivity control for zeolites modified with organic monolayers. *Microporous Mesoporous Mater.* **2022**, *337*, 111913–111920. [CrossRef]

90. Zhang, Z.Q.; Peh, S.B.; Kang, C.J.; Chai, K.G.; Zhao, D. Metal-organic frameworks for C_6–C_8 hydrocarbon separations. *J. Energy Chem.* **2021**, *3*, 100057–100099. [CrossRef]

91. Han, X.; Chen, Y.T.; Su, B.G.; Bao, Z.B.; Zhang, Z.G.; Yang, Y.W.; Ren, Q.L.; Yang, Q.W. Research Progress on Adsorption and Separation Materials for Hexane Isomers. *CIESC J.* **2021**, *72*, 3445–3465. [CrossRef]

92. Xia, H.L.; Zhou, K.; Yu, L.; Wang, H.; Liu, X.Y.; Proserpio, D.M.; Li, J. Customized Synthesis: Solvent- and Acid-Assisted Topology Evolution in Zirconium-Tetracarboxylate Frameworks. *Inorg. Chem.* **2022**, *61*, 7980–7988. [CrossRef]

93. Yu, Q.C.; Guo, L.D.; Lai, D.; Zhang, Z.G.; Yang, Q.W.; Yang, Y.W.; Ren, Q.L.; Bao, Z.B. A pore-engineered metal-organic framework with mixed ligands enabling highly efficient separation of hexane isomers for gasoline upgrading. *Sep. Purif. Technol.* **2021**, *268*, 118646–118657. [CrossRef]

94. Guo, F.A.; Wang, J.; Chen, C.L.; Dong, X.L.; Li, X.Y.; Wang, H.; Guo, P.; Han, Y.; Li, J. Linker Vacancy Engineering of a Robust FTW-type Zr-MOF for Hexane Isomers Separation. *Angew. Chem. Int. Ed.* **2023**, *62*, 202219053. [CrossRef]

95. Lal, B.; Idress, K.B.; Xie, H.M.; Smoljan, C.S.; Shafaie, S.; Islamoglu, T.; Farha, O.K. Pore Aperture Control toward Size-Exclusion-Based Hydrocarbon Separations. *Angew. Chem. Int. Ed.* **2023**, *62*, 2022190533–2022190539. [CrossRef]

96. Sun, H.; Jiang, H.; Kong, R.Q.; Ren, D.N.; Wan, D.; Tan, J.L.; Wu, D. Tuning n-Alkane Adsorption on Mixed-linker ZIF-8-90 via Controllable Ligand Hybridization: Insight into the Confinement from an Energetics Perspective. *Ind. Eng. Chem. Res.* **2019**, *29*, 13274–13283. [CrossRef]

97. Peralta, D.; Chaplais, G.; Simon, M.A.; Barthelett, K.; Pirngrubert, G.D. Separation of Cgparaffins using zeolitic imidazolate frameworks: Comparison with zeolite 5A. *Ind. Eng. Chem. Res.* **2012**, *51*, 4692–4702. [CrossRef]

98. Liu, J.C.; Yang, X.M.; Wang, C.; Ye, L.; Sun, H. Synthesis of hierarchical 5A zeolites to improve the separation efficiency of n-paraffins. *Adsorp. Sci. Technol.* **2019**, *37*, 530–544. [CrossRef]

99. Sun, H.; Sun, Z.W.; Shen, B.X.; Liu, J.C.; Li, G.N.; Wu, D.; Zhang, Y.X. One-pot synthesis of binderless zeolite A spheres via in situ hydrothermal conversion of silica gel precursor. *AICHE J.* **2018**, *64*, 4027–4038. [CrossRef]

100. Sun, H.; Shen, B.X. Experimental study on coking, deactivation, and regeneration of binderless 5A zeolite during 1-hexene adsorption. *Adsorption* **2013**, *19*, 111–120. [CrossRef]